

# 1 Observing and Modeling Earth's Energy Flows, 2 Thirteen Years Later

3 Miklos Zagoni

4 Eotvos Lorand University, Faculty of Natural Sciences, Budapest, Hungary

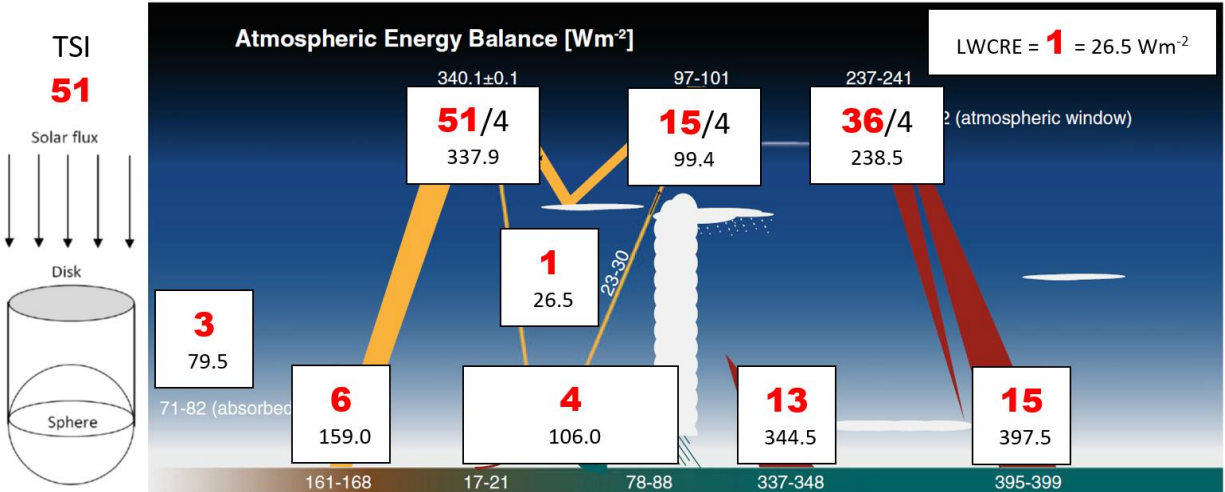
5 e-mail: miklos.zagoni@t-online.hu

6 **Abstract** Observing and modeling energy flows in Earth's climate system was reviewed in an  
7 article in *Surveys in Geophysics* thirteen years ago as a concluding paper of a special collection  
8 with the same title. Analyzing their global mean energy budget estimate, a remarkable recognition  
9 can be made: there are specific small integer ratios among the flux components, as each of them  
10 are very close to an integer multiple of a unit flux, which is the longwave cloud radiative effect  
11 (LWCRE) with a value of  $26.5 \text{ Wm}^{-2}$ , as given in that study. Similar global energy budget  
12 estimates later by other authors, the IPCC and the NASA CERES science team show the same  
13 structure with convincing accuracy: typically, within the stated ranges of uncertainty. The physical  
14 science basis for the core flux components is identified in four radiative transfer constraint  
15 equations having their origin in the long-known two-stream approximation of Schwarzschild's  
16 equation; the fundamental integer ratios are solutions of the set of these four equations.

17 **Keywords:** global mean energy flow systems; integer relationships; radiative transfer equations

## 18 Introduction

19 A review article was published in *Surveys in Geophysics* thirteen years ago as a concluding study  
20 of a special collection with the same title (Stevens and Schwartz, 2012). Projecting longwave cloud  
21 radiative effect (LWCRE) on the energy flow distribution with the given CERES value of  $26.5$   
22  $\text{Wm}^{-2}$ , it is easy to recognize that the flux components are integer multiples of that unit flux, close  
23 to the stated ranges of uncertainty; see Fig. 1.



1  
 2 **Fig. 1** Earth's global and annual mean energy flow system. Values are presented as a two-sigma range (Wm<sup>-2</sup>).  
 3 Original: Stevens and Schwartz (2012). We inserted LW CRE from their study, with their value from CERES  
 4 EBAF. Numbers in red bold typeface are expressed in the unit of 26.5 Wm<sup>-2</sup>. TOA fluxes are integers on the  
 5 intercepting cross-section disk of incoming solar radiation.

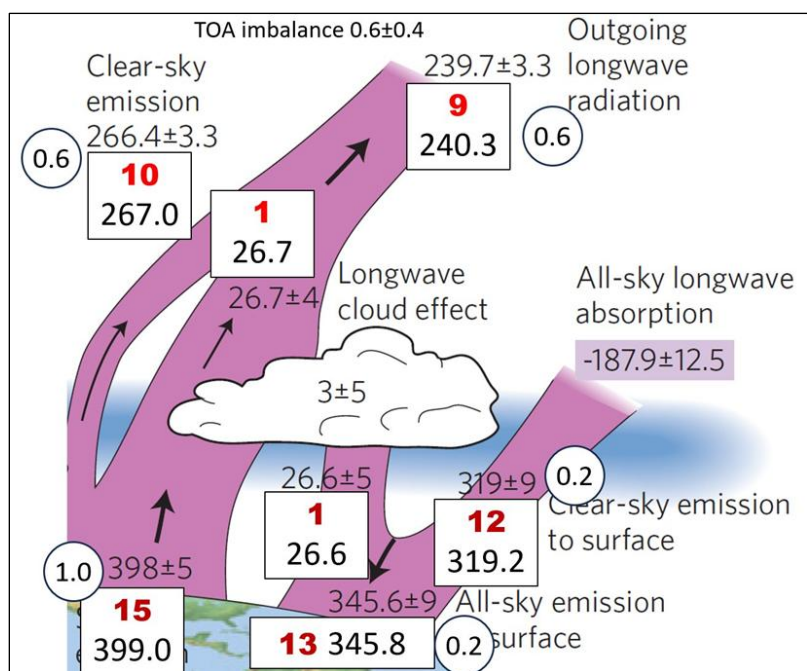
6 At the top of the atmosphere (TOA), integer positions are quarters, that is, they are integers on the  
 7 intercepting cross-section disk to incoming solar radiation, that is, before division by 4 for  
 8 spherical weighting. Incoming solar radiation is smaller than the given lower limit by 2 Wm<sup>-2</sup>.  
 9 Atmospheric window is not part of the system. At the surface, integer position for absorbed solar  
 10 radiation (6 units, with a value of 159.0 Wm<sup>-2</sup>) falls out the indicated range of 161-168.  
 11 Components of the convective flux (sensible heat and latent heat) do not fit separately into the  
 12 integer system, but their sum (4 units = 106.0 Wm<sup>-2</sup>) does. The position of total solar irradiance  
 13 (TSI) is 51 units which, using the spherical factor, would be 1351.5 Wm<sup>-2</sup>; with geodetic weighting  
 14 (factor 4.0034, as in CERES EBAF), 1352.65 Wm<sup>-2</sup>; still unacceptably low.

15 With these several exceptions, the appearance of the integer ratio system is interesting, but not  
 16 convincing; without further indication, it may be regarded as a simple coincidence.

17 But later in that year, another update on global energy balance was published, based on the then-  
 18 available best global observations (Stephens et al. 2012), where similar structures appear. First,  
 19 the longwave cloud effect at TOA was upgraded to 26.7 (±4) Wm<sup>-2</sup>, resulting in TSI = 51 units =  
 20 1361.7 Wm<sup>-2</sup> (with the spherical multiplying factor of 4), or 1362.86 Wm<sup>-2</sup> (with the geodetic  
 21 formula of 4.0034). Since the then-accepted solar irradiance value was TSI = 1360.8 ± 0.5 Wm<sup>-2</sup>  
 22 (Kopp and Lean 2011), the latter would result in TSI/51 = 26.68 Wm<sup>-2</sup> in the spherical case, and

1 26.66  $\text{Wm}^{-2}$  in real-Earth geometry, supporting the fine-tuning in LWCRE. Integer positions for  
 2 “Incoming solar” with the CERES geodetic factor of 4.0034 is  $340.14 \text{ Wm}^{-2}$ , and “Reflected solar”  
 3 is  $100.04 \text{ Wm}^{-2}$  ( $340.2$  and  $100.0$  are shown in the diagram).

4 Now with the value of  $26.7 \text{ Wm}^{-2}$ , given as the difference of “Clear-sky emission” ( $266.4$ ) and  
 5 “Outgoing longwave radiation” (all-sky emission,  $239.7$ ) in Fig. B1 of Stephens et al. (2012), these  
 6 values themselves are integer multiples of this unit flux as  $266.4 = 10 \times 26.7$  (and consequently  
 7  $239.7 = 9 \times 26.7$ ) with a difference  $0.6 \text{ Wm}^{-2}$  only, which is far within the stated range of  
 8 uncertainty (3.3), and equivalent to the indicated TOA imbalance. Similarly, at the surface, “Clear-  
 9 sky emission to surface” ( $319$ ) and “All-sky emission to surface” ( $345.6$ ) differ by the longwave  
 10 cloud effect at the surface (LWCRE SFC,  $26.6$ ), and these values are integer multiples of LWCRE  
 11 SFC, as  $319 = 12 \times 26.6$  with a difference of  $0.2 \text{ Wm}^{-2}$ , hence  $345.6 = 13 \times 26.6$  ( $- 0.2 \text{ Wm}^{-2}$ ),  
 12 compared to the stated  $\pm 9 \text{ Wm}^{-2}$  uncertainty. Finally, “Surface emission” ( $398$ ) also occupies an  
 13 integer position, as  $398 = 15 \times 26.6$ , the difference is  $1 \text{ Wm}^{-2}$ , while the indicated uncertainty range  
 14 is  $\pm 5 \text{ Wm}^{-2}$ ; the longwave part is shown in Fig. 2.



15

16 **Figure 2** The longwave part of the global annual mean energy budget of Earth (Stephens et al. 2012,  
 17 Fig.B1), with the integer system projected on it in textboxes. Red, bold typeface gives the integer values  
 18 in units of one LWCRE at TOA ( $26.7 \text{ Wm}^{-2}$ ); purple values in units of one LWCRE at the surface ( $26.6$   
 19  $\text{Wm}^{-2}$ ); the differences of the original values and the integer multiples are given in circles in  $\text{Wm}^{-2}$ .

1 Regarding the given uncertainty for LWCRE TOA as  $\pm 4 \text{ Wm}^{-2}$ , from now we will use one  
2 common unit flux for TOA and the surface.

3 Next year, another global mean energy budget distribution was presented (Wild et al. 2013), where  
4 the shortwave components were further updated, resulting in accurate positions in the integer  
5 system when using the same LWCRE TOA of  $26.7 \text{ Wm}^{-2}$  for unit flux as above. At TOA, incoming  
6 solar 340 occupies position of  $51/4 (=340.4)$ , where the division factor of four comes from  
7 spherical weighting; hence total solar irradiance  $\text{TSI} = 51 \text{ units} = 1361.7 \text{ Wm}^{-2}$ . Solar reflected  
8 (100) equals  $15/4 = 100.1$  with a difference of  $0.1 \text{ Wm}^{-2}$  only, resulting in an integer ratio for TOA  
9 albedo as  $15/51$ , being arithmetically identical to the indicated  $100/340$ . Absorbed solar and  
10 outgoing thermal radiation in equilibrium are equal with 9 units  $= 9 \times 26.7 = 240.3 \text{ Wm}^{-2}$ . Solar  
11 absorbed in the atmosphere is indicated as  $79 \text{ Wm}^{-2}$ ; an integer position is 3 units  $= 80.1 \text{ Wm}^{-2}$ ,  
12 allowing solar down to the surface  $185 \text{ Wm}^{-2}$  in the diagram and  $186.9 \text{ Wm}^{-2}$  in the integer system  
13 as 7 units; with  $161 \text{ Wm}^{-2}$  solar absorbed at the surface in the diagram and  $160.2 \text{ Wm}^{-2}$  as 6 units  
14 in the integer system. The largest difference is in “Thermal down surface”, given as  $342 \text{ Wm}^{-2}$ ,  
15 when 13 units  $= 347.1 \text{ Wm}^{-2}$ , so the bias is  $5.1 \text{ Wm}^{-2}$ , still within the noted uncertainty; see Fig. 3.

16 Even this discrepancy disappeared next year, when Loeb (2014) published a global mean energy  
17 budget based on CERES EBAF data. Refining the unit flux from  $26.7 \text{ Wm}^{-2}$  to  $26.67 \text{ Wm}^{-2}$ , the  
18 flux component “thermal down surface” (called here “Absorbed at Surface”) in the integer ratio  
19 system is  $346.7 \text{ Wm}^{-2}$ ; with a bias of  $1.7 \text{ Wm}^{-2}$  to the given value of  $345 \text{ Wm}^{-2}$ . The most peculiar  
20 feature here is that at the TOA, all three flux components (Incoming Solar, Reflected Solar and  
21 Outgoing LW Radiation) fit to their integer position with zero difference; see Fig. 4.



1 In the past decade, this higher value for the downward longwave radiation became widely  
 2 accepted. In a current assessment of the global radiation budget from a surface perspective (Li, Li,  
 3 Wild and Jones, 2024) based on 34 CMIP6 models, SW down radiation to the surface is  $186 \pm 6$ ,  
 4 Reflect by surface =  $24 \pm 3$ , convective flux (sensible heat + latent heat) = 106, Thermal down  
 5 surface =  $346 \pm 6$ , and Thermal up surface =  $402 \pm 5$  [ $\text{Wm}^{-2}$ ]. The corresponding integer positions,  
 6 with the same unit flux of  $26.67 \text{ Wm}^{-2}$  are as follows: 7 units = 186.69, 1 unit = 26.67, 4 units =  
 7 106.68, 13 units = 346.71, and 15 units = 400.05 [ $\text{Wm}^{-2}$ ]; the differences are 0.69; 2.67; 0.68; 0.71,  
 8 and 1.95 [ $\text{Wm}^{-2}$ ], respectively — each of them far within the indicated uncertainty range.

9 At the top of the atmosphere, Stackhouse et al. (2024) provide a radiation budget from CERES  
 10 satellite observations for 2001-2022. As shown in Table 1, with an upgraded unit flux of  $26.68$   
 11  $\text{Wm}^{-2}$ , the difference of their climatological mean from the integer positions falls within, or close  
 12 to (in the case of ASR), the interannual variability for the same period. Data taken from their Table  
 13 2.9.

14 **Table 1** Global mean TOA radiative fluxes (Climatological Mean and Interannual Variability) from  
 15 CERES, compared to the integer positions

Global	N	$N \times \text{unit}$ unit = $26.68$ $\text{Wm}^{-2}$	Climatological Mean 2001-22 $\text{Wm}^{-2}$	Difference $\text{Wm}^{-2}$	Interannual Variability 2001-22, $\text{Wm}^{-2}$
OLR	36/4	240.12	240.35	0.23	$\pm 0.65$
TSI	51/4	340.17	340.20	0.03	$\pm 0.15$
RSW	15/4	100.05	99.00	1.05	$\pm 1.05$
ASR	36/4	240.12	241.20	1.08	$\pm 1.05$
Net	0	0	0.85	0.85	$\pm 0.85$

16  
 17 The accuracy altogether is much better than expected from a simple coincidence, therefore an  
 18 intense quest for a possible physical science basis was initiated. Four radiative transfer equations  
 19 were identified and verified on published global energy flow distributions of CERES and GEWEX  
 20 data, from which the integer ratios for the principal components arise as a solution.

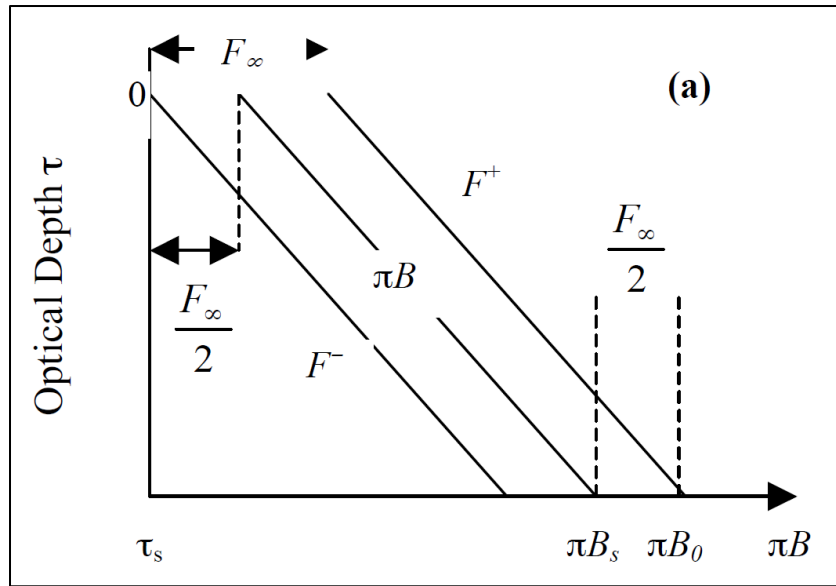
21

1 **Results**

2 The first equation is a well-known constraint on the net radiation at the surface, coming directly  
 3 from Schwarzschild’s (1906, Eq. 11) two-stream radiative equilibrium relationships ( $E$  being the  
 4 emission of the surface;  $A$  upward beam,  $B$  downward beam,  $A_0$  the emerging flux at the top-of-  
 5 atmosphere, and  $\tau$  the optical depth):

$$E = \frac{A_0}{2} (1 + \bar{\tau}), \quad A = \frac{A_0}{2} (2 + \bar{\tau}), \quad B = \frac{A_0}{2} \bar{\tau}. \quad (11)$$

7 reproduced in standard university textbooks like Goody (1964, Eq. 2.115); Houghton (1977, 1986,  
 8 2002, Eq. 2.13); Chamberlain (1978, 1987, Eq. 1.2.29 and Fig.1.4); Goody and Yung (1989,  
 9 Eq.2.146); Hartmann (1994, 2016, Eqs. 3.48-3.54); Salby (1996, 2012, Eq. 8.67); Pierrehumbert  
 10 (2008, Eq. 4.45); Ambaum (2021, Eq. 10.56), and in university lecture notes (Stephens 2003), for  
 11 example as  $\pi B_s - \pi B_0 = F_{\infty}/2$ , see Fig.5.



12  
 13 **Figure 5** The flux profiles and blackbody function predicted by the simple gray body model as a function  
 14 of optical depth (Stephens 2003)

15 The middle and third terms in Schwarzschild’s (1906, Eq. 11) for the upward and downward beam  
 16 were also reproduced in identical form in Stephens et al. (1994). The difference of the second and  
 17 first terms in Schwarzschild (1906, Eq. 11) results the net radiation at the surface, representing a

1 temperature discontinuity in radiative equilibrium, being “*greatly diminished by convection and*  
2 *heat conduction*”, as noted by Emden (1903). Authors generally note that “*such a steep lapse rate*  
3 *is very unstable with respect to vertical motion, and will soon be destroyed by the process of*  
4 *convection*” (Houghton 1977), “*such discontinuities are usually are greatly suppressed in reality*  
5 *because of efficient heat transport by conduction and convection*” (Hartmann 1994), also “*This*  
6 *temperature discontinuity is unstable in practice and there will be turbulent heat exchange which*  
7 *will remove the temperature discontinuity*” (Ambaum 2021).

8 The equation states that the net radiation at the surface ( $R_N$ ) in radiative equilibrium — and the  
9 corresponding convection in radiative-convective equilibrium — is independent of the optical  
10 depth and equals half of the outgoing longwave radiation (OLR) in the clear-sky:

11 Eq. (1)  $R_N$  (clear-sky) = SFC (SW net + LW net) (clear-sky) = (SW down – SW up) + (LW down  
12 – LW up) (clear-sky) = OLR (clear-sky)/2.

13 As an initial justification, the equation was controlled on the then-available NASA CERES dataset,  
14 Energy Balanced and Filled (EBAF-Surface) Edition 2.8. Data were taken from the Data Quality  
15 Summary (2015).

16 Eq. (1) CERES\_EBAF-Surface Ed2.8, Table 4.1

17  $R_N$  (clear-sky) = SW down – SW up + LW down – LW up (clear-sky) = OLR(clear-sky)/2.

18 
$$243.9 - 29.7 + 316.0 - 398.0 = 265.7/2 - 0.65$$

19 The equation is valid on that data product with a difference of  $0.65 \text{ Wm}^{-2}$ . [Note that Earth’s heat  
20 uptake in that time was estimated as  $0.58 \pm 0.38 \text{ Wm}^{-2}$  (Loeb et al. 2012).]

21 Since the first equation prescribes the convective flux (the sum of the sensible heat flux and latent  
22 heat flux) in a direct relationship to the outgoing longwave radiation (OLR) at TOA in the clear-  
23 sky, and convection changes almost linearly with sea surface temperature, a definite OLR-  
24 dependent convection assumes a definite, OLR-dependent surface upward longwave (ULW)  
25 thermal emission. Exploring possible formulas, as the optical depth ( $\tau$ ) of zero defines TOA, and  
26  $\tau = 1$  the level where OLR is initiated, Schwarzschild’s formula for the surface (the middle term

1 in Eq. 11) was tried at  $\tau = 2$ . Then the second equation gives the total SW + LW absorbed radiation  
2 ( $R_T$ ) at the surface in the clear-sky:

3 Eq. (2)  $R_T$  (clear-sky) = (SW down – SW up + LW down) (clear-sky) = 2OLR(clear-sky).

4 CERES EBAF-Surface Ed2.8 Data Quality Summary (DQS) data [17]:

5  $243.9 - 29.7 + 316.0 = 2 \times 265.7 - 1.2 \text{ Wm}^{-2}$ .

6 This accuracy (compared to the estimated uncertainties in the EBAF-Surface data of  $1\sigma$  between  
7 3 and 7  $\text{Wm}^{-2}$ , see Table 4.2 of [17]) was convincing enough to proceed further in this direction.

8 For all-sky, a third and fourth equations were created from the first pair, by separating atmospheric  
9 radiation transfer from the longwave effect of clouds (LWCRE) and using all-sky data on both  
10 sides:

11 Eq. (3)  $R_N$  (all-sky) = Surface SW net + LW net (all-sky) = [OLR(all-sky) – LWCRE]/2;

12 and

13 Eq. (4)  $R_T$  (all-sky) = Surface (SW + LW) absorbed (all-sky) = (SW down – SW up + LW down)  
14 (all-sky) = 2OLR (all-sky) + LWCRE.

15 Their accuracy on that data product was  $2.65 \text{ Wm}^{-2}$  for Eq. (3) and  $2.10 \text{ Wm}^{-2}$  for Eq. (4).

16 Controlled the four equations on EBAF Ed4.1\_V3 and Ed4.2\_V4 data products, we have the biases  
17 of the individual equations are within the range of  $\pm 2.83 \text{ Wm}^{-2}$ ; and the mean bias of the four  
18 equations is  $0.0007 \text{ Wm}^{-2}$  (this justifies the use of four decimal places in the netCDF file), see  
19 Table 2, shown in green. EBAF Edition 4.2 is also controlled; with Version 4 data, first on the  
20 same period (April 2000-March 2022); the differences become as follows: -2.35, -2.70, 3.98, 3.46;  
21 the mean bias is  $0.60 \text{ [Wm}^{-2}]$  (red); then on the extended time period April2000-March 2024  
22 (brown), and have -2.32, -2.50, 4.01, 3.67, with a mean of  $0.715 \text{ [Wm}^{-2}]$ , still far within the  
23 absolute calibration uncertainty of the CERES instrument, and in the magnitude of the estimated  
24 Earth's Energy Imbalance.

25

1 **Table 2** The four equations controlled on CERES EBAF Ed4.1 (April 2000 – March 2022) and Ed4.2  
 2 (April 2000 – March 2022, and April 2000 – March 2024) data

CERES EBAF Ed4.1 Version 3, 22 years (April 2000 – March 2022) (Wm <sup>-2</sup> )			
CERES EBAF Ed4.2 Version 4, 22 years (April 2000 – March 2022) (Wm <sup>-2</sup> )			
CERES EBAF Ed4.2 Version 4, 24 years (April 2000 – March 2024) (Wm <sup>-2</sup> )			
Eq. (1)	SFC SW down – SW up + LW down – LW up (clear) = TOA LW (clear)/2		
	240.8680 – 29.0724 + 317.4049 – 398.5211	= 266.0122 /2	– 2.3267
	241.0969 – 29.7521 + 317.8744 – 398.5890	= 265.9594 /2	– 2.3495
	241.0514 – 29.7043 + 318.0984 – 398.7742	= 265.9748 /2	– 2.3161
Eq. (2)	SFC SW down – SW up + LW down (clear) = 2 × TOA LW (clear)		
	240.8680 – 29.0724 + 317.4049	= 2 × 266.0122	– 2.8238
	241.0969 – 29.7521 + 317.8744	= 2 × 265.9594	– 2.6996
	241.0514 – 29.7043 + 318.0984	= 2 × 265.9748	– 2.5042
Eq. (3)	SFC SW down – SW up + LW down – LW up (all) = [TOA LW (all) – LWCRE]/2		
	186.8544 – 23.1629 + 345.0108 – 398.7550	= (240.2450 – 25.7672)/2	+ 2.7083
	187.1451 – 23.4950 + 346.1057 – 398.4220	= (240.3317 – 25.6277)/2	+ 3.9818
	187.1756 – 23.4607 + 346.3158 – 398.6162	= (240.3894 – 25.5854)/2	+ 4.0126
Eq. (4)	SFC SW down – SW up + LW down (all) = 2 × TOA LW (all) + LWCRE		
	186.8544 – 23.1629 + 345.0108	= 2 × 240.2450 + 25.7672	+ 2.4450
	187.1451 – 23.4950 + 346.1057	= 2 × 240.3317 + 25.6277	+ 3.4647
	187.1756 – 23.4607 + 346.3158	= 2 × 240.3894 + 25.5854	+ 3.6665
		Mean	0.0007
			0.5994
			0.7147

3  
 4 This unprecedented accuracy of the constraint equations raises a couple of questions. Do these  
 5 four equations express an arithmetic identity? The answer is no; in the prevailing theory we are  
 6 not aware of any relationship that would require these couplings between surface and TOA  
 7 irradiances, without referring to any atmospheric gaseous composition or the optical depth. Or, are  
 8 these four equations built in the CERES data production protocol? No again: the mean bias in the  
 9 first five years vary between -0.5 and -0.2 [Wm<sup>-2</sup>] and it approaches zero after including 17 years  
 10 into the averaging; then it occupies the value of zero and remains there after only two decades.

11 Notice that the clear-sky equations prescribe the ratio

12  $R_N : (TOA\_LW\_up) : (SFC\_LW\_up) : R_T = 1 : 2 : 3 : 4 ,$

13 resulting in a clear-sky greenhouse factor of

14  $g(\text{clear-sky}) = G(\text{clear-sky}) / (SFC\_LW\_up) = [(SFC\_LW\_up) - (TOA\_LW\_up)] / (SFC\_LW\_up)$   
 15  $= 1/3.$

1 With CERES EBAF Edition 4.2 V4 (24-yr) data (Table 1),  $g(\text{clear-sky, CERES}) = (398.7742 -$   
 2  $265.9748) / 398.7742 = 0.3330$ .

3 Recently, data were published from global energy and water cycle assessments on 30 years of the  
 4 GEWEX mission (Stephens et al. 2023). Their data are for all-sky, therefore only equations (3)  
 5 and (4) maybe controlled, with LWCRE taken from an earlier study of the same authors (Stephens  
 6 et al. 2012) as  $26.7 \text{ Wm}^{-2}$ . According to Fig. 2 of the GEWEX study, net radiation at the surface  
 7 (R) equals the sum of the convective fluxes: latent heat (evaporation) and sensible heat. Using data  
 8 from Fig. SB3,

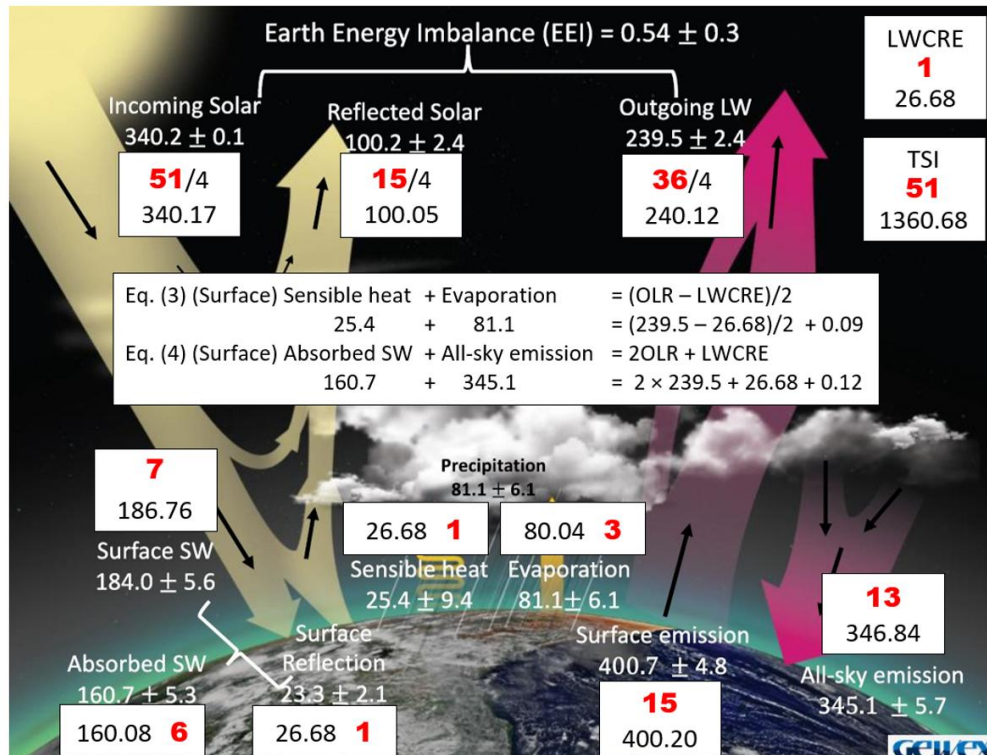
9 Eq. (3)  $R_N = LE + H = \text{"Evaporation"} + \text{"Sensible heat"} = (\text{"Outgoing LW"} - \text{LWCRE})/2$

10  $81.1 + 25.4 = (239.5 - 26.7)/2 + 0.1 [\text{Wm}^{-2}]$

11 Eq. (4)  $R_T = \text{"Surface SW"} - \text{"Surface Reflection"} + \text{"All-sky emission"} = 2 \times \text{"Outgoing LW"} +$   
 12  $\text{LWCRE}$

13  $184.0 - 23.3 + 345.1 = 2 \times 239.5 + 26.7 + 0.1 [\text{Wm}^{-2}]$

14 On GEWEX data, both the all-sky equations are valid within  $0.1 \text{ Wm}^{-2}$ ; see Fig. 6.

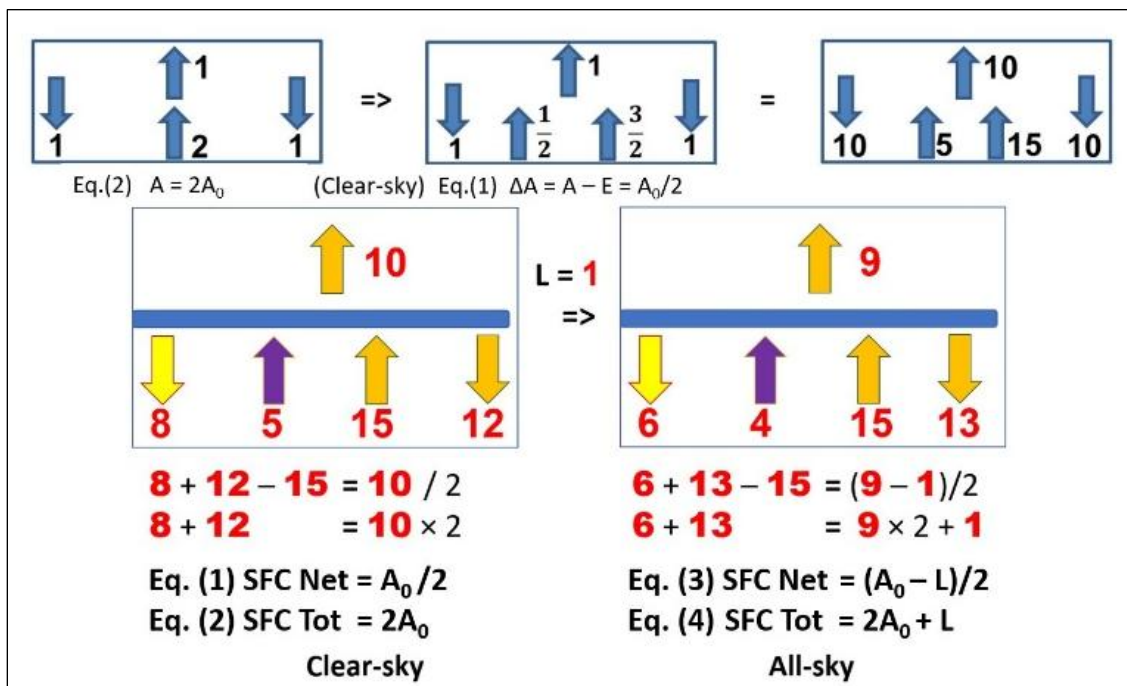


15

1 **Figure 6** The all-sky (third and fourth) equations and the integer structure is projected on the GEWEX  
 2 dataset, based on 30 years of data collection (Stephens et al. 2023). The unit flux of LWCRE is a refined  
 3 value from  $26.7 \text{ Wm}^{-2}$  from Stephens et al. (2012) to  $26.68 \text{ Wm}^{-2}$  as the most accurate fit to TSI.

4 **Discussion: The integer solution**

5 As the equations are not direct functions of  $\tau$ , a stationary (geometric) representation may be  
 6 applied (Fig.7). Let's start with the second equation, stating the equality of the total energy  
 7 absorbed (and emitted) by the surface to twice the OLR under clear-sky. This case is described by  
 8 the simplest greenhouse model, see for example Hartmann (1994, Fig. 2.3), representing the flux  
 9 ratios of  $A = 2A_0$  [in Schwarzschild's (1906, Eq. 11) notation] as shown in the upper left panel;  
 10 Equation (1) is represented in the upper middle panel as  $\Delta A = A - E = A_0/2$  and  $E = (3/2)A_0$  (for  
 11 its simple derivation, see Hartmann 1994, Fig. 3.11 and Eq. 3.54). In the right panel of the upper  
 12 row, the ratios are the same as in the middle, multiplied by 10 (since the unit is not specified yet).  
 13 Then, introducing the red unit (for LWCRE), and keeping in mind that if Upward LW at TOA is  
 14 10 units (of LWCRE) in the clear-sky, then it must be 9 units in the all-sky; and if Downward LW  
 15 is 12 units in the clear-sky, then it will be 13 units in the all-sky, with the constraint that Upward  
 16 LW at the surface is the same in both cases, we have an integer ratio system, as shown in Fig.7.



1 **Figure 7** Stationary (geometric) representation of the four equations, with integer solution as multiples of  
 2 the unit flux of L (representing LWCRE).

3 Validity of equations and the extended set of the integers on CERES data are given in Table 3.  
 4 The fit of components not included in the equations (for example, TOA SW up both in clear-sky  
 5 and all-sky) is remarkable. Notice also that the components of convection in the GEWEX study  
 6 (based on the NEWS – NASA Energy and Water-cycle Study methodology (L’Ecuyer et al. 2015)  
 7 occupy integer positions separately.

8 **Table 3** The four equations and the integer positions for the clear-sky and all-sky global mean energy  
 9 flow system, including TSI, using the unit flux of  $26.68 \text{ Wm}^{-2}$  as the best fit on CERES EBAF Ed4.2 data,  
 10 and the differences. The greenhouse effect is also shown.

**Data: CERES EBAF Ed4.2 Version 2, October 2000 – September 2023**

Eq. (1)  $8 + 12 - 15 = 10/2$ ; Eq. (2)  $8 + 12 = 10 \times 2$ ;  
 Eq. (3)  $6 + 13 - 15 = (9 - 1)/2$ ; Eq. (4)  $6 + 13 = 9 \times 2 + 1$        $1 = 26.68 \text{ Wm}^{-2}$

TSI = <b>51</b> Clear-sky	<b>N</b>	<b>N</b> × Unit ( $\text{Wm}^{-2}$ )	EBAF Ed4.2 ( $\text{Wm}^{-2}$ )	Diff ( $\text{Wm}^{-2}$ )
TOA LW up	<b>40</b> /4	266.80	265.95	-0.85
TOA SW up	<b>8</b> /4	53.36	53.78	0.42
TOA SW net	<b>3</b> /4	20.01	20.47	0.46
SFC SW net	<b>8</b>	213.44	211.33	-2.11
SFC LW down	<b>12</b>	320.16	318.06	-2.10
SFC LW up	<b>15</b>	400.20	398.58	-1.62
G	<b>5</b>	133.40	132.63	-0.77
<b>TSI = 51 All-sky</b>				
TOA LW up	<b>36</b> /4	240.12	240.37	0.25
TOA SW up	<b>15</b> /4	100.05	98.95	-1.10
SFC SW net	<b>6</b>	160.08	163.71	3.63
SFC LW down	<b>13</b>	346.84	346.25	-0.59
SFC LW up	<b>15</b>	400.20	398.75	-1.45
G	<b>6</b>	160.08	158.38	-1.70

11  
 12 Let us call here an independent estimate of the clear-sky greenhouse effect from the GFDL  
 13 Atmospheric Model 4 (Raghuraman et al. 2019), showing its value as  $133.4 \pm 0.6 \text{ Wm}^{-2}$ . Notice  
 14 that the clear-sky greenhouse factor is  $g(\text{clear-sky}) = G / \text{SFC LW up} = 5/15 = 1/3$  in the integer  
 15 system and  $132.63/398.58 = 0.333$  with CERES data. The integer position for the all-sky  
 16 greenhouse factor is  $g(\text{all-sky}) = 6/15 = 0.4$ , while CERES data gives  $158.38/398.75 = 0.397$ .

## 1 **References**

- 2 Ambaum, M. H. P. *Thermal Physics of the Atmosphere*. Royal Meteorological Society (2021).
- 3 Andrews, D. *An Introduction to Atmospheric Physics*. Cambridge University Press (2010).
- 4 Chamberlain, J. *Theory of Planetary Atmospheres*. Academic Press (1978) (2<sup>nd</sup> edition: 1987).
- 5 Emden, R. (1913) Über Strahlungsgleichgewicht und atmosphärische Strahlung.  
6 Sitzungsberichte der mathematisch-physikalischen Klasse der Königlich Bayerischen Akademie  
7 der Wissenschaften zu München. English translation: Radiation equilibrium and atmospheric  
8 radiation, by H. Bateman. Monthly Weather Review (1916).
- 9 Goody, R. *Atmospheric Radiation: Theoretical Basis*. Oxford University Press (1964, 2<sup>nd</sup> edition  
10 with Y.L.Yung, 1989).
- 11 Hartmann, D. *Global Physical Climatology*. Academic Press. (1994). (2<sup>nd</sup> edition: 2016).
- 12 Houghton, J. *The Physics of Atmospheres*. Cambridge University Press (1977).
- 13 Kopp, G. and J. Lean, A new, lower value of total solar irradiance: Evidence and climate  
14 significance. *GRL* **38**, L01706 (2011), <https://doi.org/10.1029/2010GL045777>
- 15 L'Ecuyer, T. S., and Coauthors, The Observed State of the Energy Budget in the Early Twenty-  
16 First Century, *J. Climate*, **28**, 8319–8346 (2015) <https://doi.org/10.1175/JCLI-D-14-00556.1>.
- 17 Li, X., Q. Li, M. Wild, P. Jones (2024) An intensification of surface Earth's energy imbalance  
18 since the late 20<sup>th</sup> century. *Nature Comm. EE*, 30 Oct 2024.
- 19 Loeb, N., Lyman, J., Johnson, G. *et al.* Observed changes in top-of-the-atmosphere radiation and  
20 upper-ocean heating consistent within uncertainty. *Nature Geosci* **5**, 110–113 (2012).  
21 <https://doi.org/10.1038/ngeo1375>
- 22 NASA CERES CERES\_EBAF-Surface\_Ed2.8 Data Quality Summary (March 27, 2015).
- 23 NASA CERES EBAF Ed4.1\_V3 and Ed4.2\_V4.
- 24 Pierrehumbert, R., *Principles of Planetary Climate*. Cambridge University Press (2008).

1 Raghuraman, S. P., Paynter, D., & Ramaswamy, V. (2019). Quantifying the drivers of the clear  
2 sky greenhouse effect, 2000–2016. *Journal of Geophysical Research: Atmospheres*, 124, 11354–  
3 11371. <https://doi.org/10.1029/2019JD031017>,

4 Salby, M., *Fundamentals of Atmospheric Physics*. Academic Press (1996).

5 Salby, M., *Physics of the Atmosphere and Climate*. Cambridge University Press (2012).

6 Schwarzschild, K. (1906) Ueber das Gleichgewicht der Sonnenatmosphäre. Nachrichten von der  
7 Königlichen Gesellschaft der Wissenschaften zu Göttingen. Mathematisch-physikalische Klasse,  
8 pp. 41-53, Eq. 11. English translation: Menzel, D. H. (ed), *Selected Papers on the Transfer of*  
9 *Radiation* Dover Publ. (1966)

10 Stackhouse, P. et al. (2024) State of the Climate in 2023; *Bull. Am. Met. Soc.*, August 2024.

11 Stephens, G. (2003) Colorado State University AT622 Section 6, Eqs. (6.10a)-(6.10b), Example  
12 6.3, Fig. 6.3a.  
13 [https://reef.atmos.colostate.edu/~odell/AT622/stephens\\_notes/AT622\\_section06.pdf](https://reef.atmos.colostate.edu/~odell/AT622/stephens_notes/AT622_section06.pdf)

14 Stephens, G., Li, J., Wild, M. *et al.* An update on Earth's energy balance in light of the latest  
15 global observations. *Nature Geosci* **5**, 691–696 (2012). <https://doi.org/10.1038/ngeo1580>

16 Stephens, G. L., Slingo, A., Webb, M. J., Minnett, P. J., Daum, P. H., Kleinman, L., ... &  
17 Randall, D. A. (1994). Observations of the Earth's Radiation Budget in relation to atmospheric  
18 hydrology: 4. Atmospheric column radiative cooling over the world's oceans. *Journal of*  
19 *Geophysical Research: Atmospheres*, 99(D9), 18585-18604.

20 Stephens, G., and Coauthors, (1994) The First 30 Years of GEWEX. *Bull. Amer. Meteor.*  
21 *Soc.*, **104**, E126–E157, <https://doi.org/10.1175/BAMS-D-22-0061.1>.

22 Stevens, B., Schwartz, S. (2012) Observing and Modeling Earth Energy flows. *Surv Geophys*  
23 33:779-816

24 Wild, M., Folini, D., Schär, C. *et al.* The global energy balance from a surface perspective. *Clim*  
25 *Dyn* **40**, 3107–3134 (2013). <https://doi.org/10.1007/s00382-012-1569-8>